Check for
updates

Double layer silica antireflective films with high strength and rub resistance prepared by sol gel method

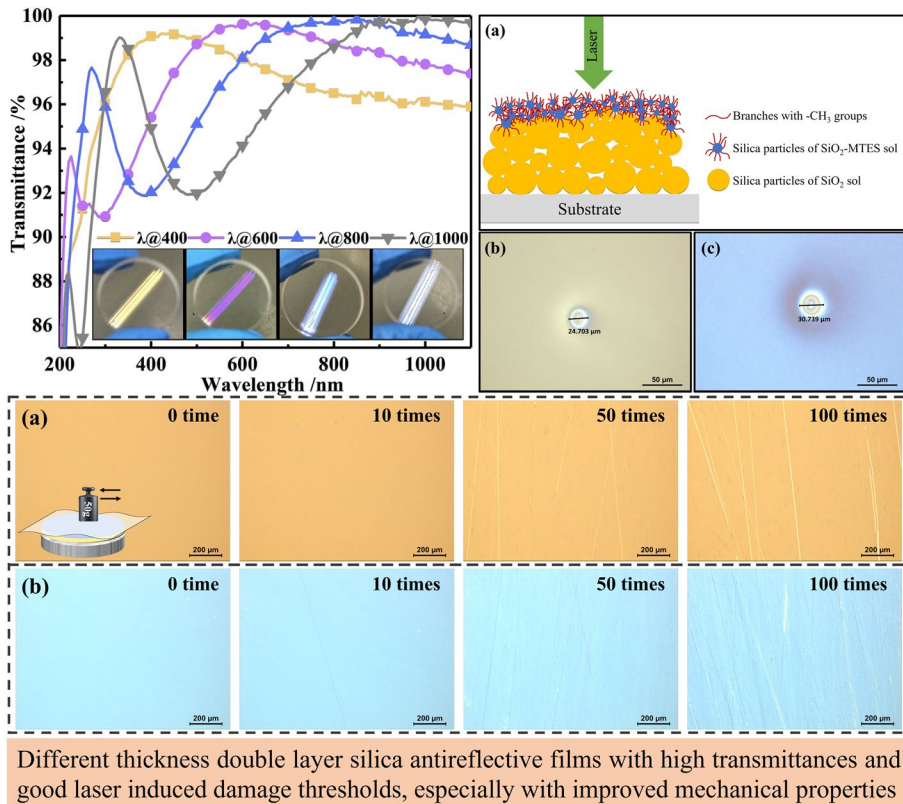Bin Shen[1,2] · Xu Zhang[1] · Haiyuan Li[1] · Xinglong Xie[1,2]

Abstract

The single-layer silica antireflective film with base catalysis prepared by sol gel method is an important part of the high-power laser facility for inertial confinement fusion, while the weak adhesion between the single-layer silica film and the substrate during the preparation process makes it susceptible to be contacted erasure and unable to be used. Double-layer silica antireflective (DLAR) films of different thicknesses were obtained using the base catalysis sol–gel method, in which the upper layer was coated with a relatively dense thin layer, and the performances of the films were characterized. The results showed that the transmittances of the DLAR films with different thicknesses were ˃99.0%, and in which one of the maximum transmittance peaks reached to 99.83% @ 1000 nm. The surface roughness of the DLAR films was < 2.0 nm, and the surfaces of the films were flat. The contact angles between DLAR films and water reached 118° and maintained stable in high humidity environment. The laser induced damage thresholds for different thickness DLAR films (peak transmittances @ 400, 600, 800, 1000 nm) were comparable to device requirements by 1-on-1 testing method, and the DLAR films exhibited high strength and good friction resistance.

✉ Bin Shen
  bingo2011@siom.ac.cn

1   Key Laboratory of High Power Laser and Physics, Shanghai Institute of Optics and Fine
    Mechanics, Chinese Academy of Sciences, Shanghai 201800, China

2   Center of Materials Science and Optoelectronics Engineering, University of Chinese Academy
    of Sciences, Beijing 100049, China

Graphical abstract

Different thickness double layer silica antireflective films with high transmittances and good laser induced damage thresholds, especially with improved mechanical properties

1 Introduction

Sol–gel technology, in which tetraethoxysilane (TEOS) is used as a precursor, was discovered by J. J. Ebelmen in 1846, and a new era of sol–gel chemistry was created(Aegerter 2011). Over time, the sol–gel technology has been further developed and widely used to prepare various materials, including films(Shen et al. 2022; Dong et al. 2024; Zhao et al. 2023), fibers(Chen et al. 2022; Barton et al. 2023), and ceramics(Tran et al. 2022; Cruz et al. 2022). Antireflective films, made of thin-film materials, are widely applied in daily life, military science, electronics, and other fields. Silica antireflective films with excellent properties, prepared by the base catalysis sol–gel method (SiO_2-ARB), are popularly used in the terminal components of high-power laser facilities (HPLFs), including fused silica glasses and potassium dihydrogen phosphate crystals. Silica antireflective films exhibit a particle-stacking structure with a low refractive index, high porosity, and high laser induced damage threshold (LIDT). These films can effectively help achieve a specific optical wavelength antireflection when combined with optical components. However, the

SiO_2-ARB films, with several times higher LIDTs, are more easily erased and damaged than the films prepared using the physical vapor deposition method(Yuan et al. 2017; Peng et al. 2014). This is because the SiO_2-ARB films only adhere to the surface of substrates by adhesive forces with poor compactness. During the coating process of SiO_2-ARB films, by using the clamping process of coating elements, the film layers are prone to injury. This will affect the normal use of the elements in future studies.

Many researchers have attempted to enhance the film strength to solve the problem of low bonding surface strength between the SiO_2-ARB and substrate. Avice et al.*(*Avice et al. 2023; Boudot et al. 2014) improved the mechanical properties of silica antireflective films through vapor-phase ammonia curing; however, the damage caused to the films by wiping could not be completely avoided. Li et al.(Li and Shen 2011; Ye et al. 2019) prepared double-layer high-strength silica films by acid catalysis; however, the LIDT of the films was not be considered owing to the sol properties of the random linear chain structure winding. Ye et al.*(*Ye et al. 2011) studied the preparation of antireflective coatings with enhanced abrasion resistance using a base/acid two-step catalyzed sol–gel process. The transmittance of these films was lower than that required for HPLFs. Nevertheless, few researchers attempted to improve the mechanical strength of SiO_2-ARB while ensure its key performances suitable for HPLFs. Sun et al.(Sun et al. 2015) prepared the broadband antireflective coating exhibited strong mechanical performance and good environmental stability which was very useful for various types of solar cells. It is needed for inertial confinement fusion to make a research of high-strength double-layer silica antireflective (DLAR) films on substrates prepared using base catalysis processes.

In this study, a relatively thin dense film layer was added on the surface of the pore structure to enhance the strength of the whole film layer while maintaining the bottom base catalysis film layer skeleton. This skeleton was built on the mature sol gel antireflective film technology used in "Shenguang II" (SG II) HPLF. Various properties of the films were studied and an ideal double-layer, high-strength, friction-resistant antireflective film was obtained.

2 Experiments

2.1 Preparation of sols

Silica sol preparation for bottom layer film (SiO_2-BASE sol): A mature silica sol preparation process with base catalysis for antireflective films was applied to SG II HPLF to prepare the SiO_2-BASE sol(Shen et al. 2022, 2016). TEOS, ethanol (EtOH), ammonia (NH_3), deionized water (H_2O), and polyethylene glycol (PEG200) were mixed in a molar ratio of $1:34.2:0.9:2:0.08$ and stirred. The mixed solution was constantly stirred at 5 and 20 ℃ for approximately 5 and 2 h for hydrolysis and condensation reactions. Then, the sealed solution was aged for 8 d in a 50 ℃ oven and refluxed for ammonia removal to obtain SiO_2-BASE sol, which could be used for coating.

Silica sol preparation for up-layer film (SiO_2–MTES sol)(Shen et al. 2024): The preparation diagram of SiO_2–MTES sol was shown in Fig. 1, methyltriethoxysilane (MTES) with hydrophobic groups was added to prepare the modified silica sol for upper layer coating using a step-by-step solution preparation method. TEOS, EtOH, NH_3, and H_2O in a molar ratio of $1:23.7:0.8:1.4$ (sol 1) and TEOS, EtOH, NH_3, H_2O, and PEG200 in a molar ratio of $1:23.7:0.8:1.4:0.08$ (sol 2) were mixed and stirred, similar to SiO_2-BASE sol, for a period;
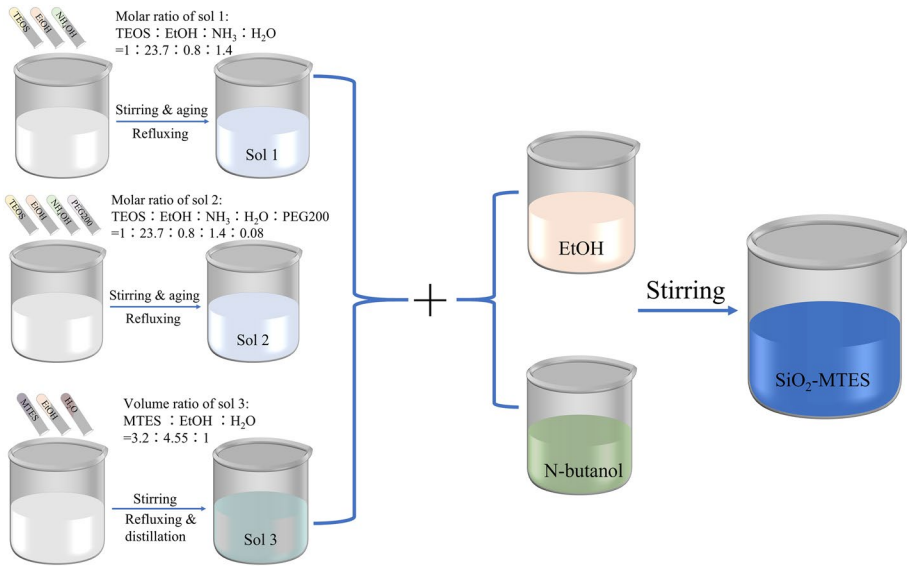
Fig. 1 Preparation diagram of SiO$_2$-MTES

both the solutions were then aged for 21 d and 14 d in a 50 ℃ oven, respectively. Sol 1 and sol 2 were obtained after refluxing (ammonia removal). MTES, EtOH, and H$_2$O were mixed in a volume ratio of 3.2:4.55:1 to conduct a chemical reaction. A colorless transparent solution (sol 3) was obtained after refluxing and distillation. Finally, sol 1, sol 2, sol 3, EtOH, and n-butanol were blended in a volume ratio of 2:1:1:5:1 to obtain the SiO$_2$–MTES sol for the upper layer coating.

2.2 Preparation of films

Fused silica optics are the main optical materials used in the terminal components of HPLFs(Zhu et al. 2019). In a custom-made dip-coating machine, φ32 mm×7 mm (φ: diameter) JGS1 substrates cleaned with ethanol were successively immersed in sol 1 and sol 2 to coat the bottom- and upper-layer films, respectively. The substrates were then pulled out at a speed of 0.3–3 mm/s for bottom layer film and slower speed for up layer film. Each layer of film was coated and left to stand for over 12 h and then subjected to 180 ℃/24 h heat treatment in an oven. Different antireflective films with peak transmittances near 400, 600, 800, and 1000 nm were obtained on JGS1 fused silica substrates (λ@400, λ@600, λ@800, and λ@1000) whose optical thickness was a quarter of the center wavelength (about 100, 150, 200, 250 nm separately) based on optical principle(Chi et al. 2020; Liu and Yeh 2010), and the dip coating speed of bottom layer film is 0.4, 0.8, 1.25, 1.75 mm/s, separately.

3 Results and discussion

The thickness of a sol–gel chemical film prepared by dip coating is affected by the concentration of the solution, pulling speed, and surface tension of the solution. The final film thickness satisfied the Landau–Levich equation as follows(Aegerter and Menning 2004),

$$h = c \cdot \frac{(\eta U)^{\frac{2}{3}}}{\gamma^{\frac{1}{6}}(\rho g)^{\frac{1}{2}}} \qquad (1)$$

where h is the thickness of the film; U is the substrate withdrawal speed; η、ρ、γ are the viscosity, density, and surface tension of the solution, respectively; g is the gravitational acceleration; c is a constant of Newtonian fluids. Viscosity is an important variable that determines whether the film can be formed and the uniformity of the film after formation. The viscosity can indirectly reflect the reaction degree of the sol. If the viscosity of sol is too small, the reaction is not sufficient, and if the viscosity is too large, it is difficult to deposit a uniform film(Jiang et al. 2017). Meanwhile, it has a direct effect on the porosity of antireflective films by controlling particle size distribution (PSD)(Tamar et al. 2016).The viscosities and PSD test results of the SiO_2-BASE sol and SiO_2-MTES sol measured using an ARES G2 rheometer (TA, USA) and a Nano ZS particle size analyzer (Malvern, Britain) are shown in Fig. 2. As shown in Fig. 2a, a linear relationship was observed between the shear force and shear rate during the viscosity measurement of the sols. The viscosities of SiO_2-BASE and SiO_2-MTES were 1.61×10^{-3} and 1.72×10^{-3} Pa·s, respectively, and changed slightly with an increase in the shear rates. These two sols with ethanol as a solvent had a small solid content and could be considered Newtonian fluids, suitable for the pulling method coating at different speeds. As shown in Fig. 2b, the PSD of the SiO_2-BASE sol used for the bottom layer was significantly larger than that of the SiO_2–MTES sol, and the peak PSD diameters of the SiO_2-BASE and SiO_2–MTES sols were 48.61 and 17.88 nm, respectively. The chemical reagent MTES is a prepolymer with chain-like molecular structures. It was used in the formation of a SiO_2–MTES sol with a large number of small silica spheres in the branched chain. Therefore, some surface-membrane particles penetrated the pores of the bottom membrane and formed a dense composite membrane on the surface, which enhanced the surface strength of the film.
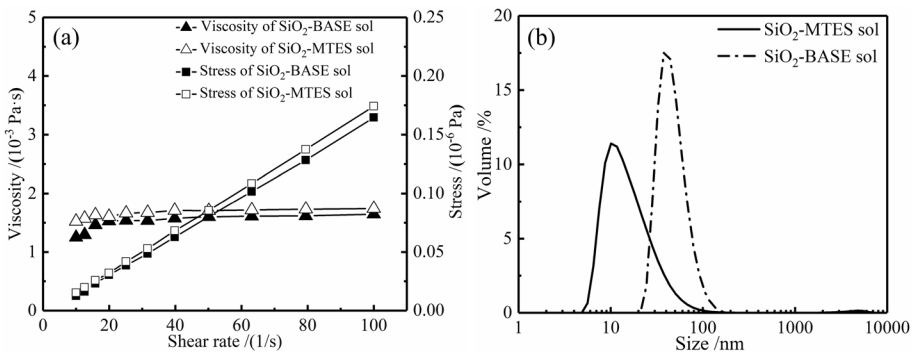

Fig. 2 Properties of sols: **a** viscosities; **b** PSD

The final optics assemblies used in target chamber of HPLFs are usually coated with sol–gel antireflective films which could realize optical enhancement at specific wavelengths. The optical transmittances of different uniform DLAR films tested using a Lambda900 spectrophotometer (PerkinElmer, USA) are illustrated in Fig. 3. The transmittance peaks of λ@400, λ@600, λ@800, and λ@1000 were observed to be greater than 99%, among which the peak transmittance of the λ@1000 film reached to 99.83%; also, the antireflective effect of the films was excellent. The transmittance enhancement values of the films with different thicknesses prepared using these two sols exceeded 5% compared with the blank substrates. For λ@400, a thinner top layer film (SiO$_2$-MTES film) was needed to match the bottom layer film (SiO$_2$-BASE film) and substrate to enhance the transmittance. It is because of a mismatch caused by a significant change in refractive index of the optical components and film materials in the near ultraviolet region. In addition, sol particle infiltration probably occurred at the interface of the bilayer film during coating and heat treatment, which had a significant impact on the optical properties of the films.

Meanwhile, the thickness and refractive index of different uniform DLAR films were measured by a L116 ellipsometer (Gaertner, USA), the morphology of film cross-section was obtained by HORIBA EMAX mics2 scanning electron microscope (Hitachi, Japan), which were showed in Fig. 4 and Table 1. The porosity of DLAR films could be estimated according to the following expression(Chi et al. 2020),

$$\text{Porosity} = 1 - \frac{(n^2 - 1)(n_d^2 + 2)}{(n^2 + 2)(n_d^2 - 1)}, \tag{2}$$

where n is the refractive index of the resultant coating and $n_d = 1.46$ is the refractive index of bulk SiO$_2$. It could be seen that the refractive index of DLAR films decreased with the increase of SiO$_2$-BASE film dip coating speed, while the porosity was opposite. The thickness of SiO$_2$-BASE film was increased when the withdrawing velocity of substrates was higher, and the proportion of SiO$_2$-BASE film in DLAR films was larger. Therefore, when SiO$_2$-BASE film was thicker, SiO$_2$-MTES film could not fully penetrate into SiO$_2$-BASE film, and DLAR films still maintained the high porosity.

The coated optical components are affected by environmental changes when used in HPLFs, and one of the main influencing factors is the humidity change in the environment.
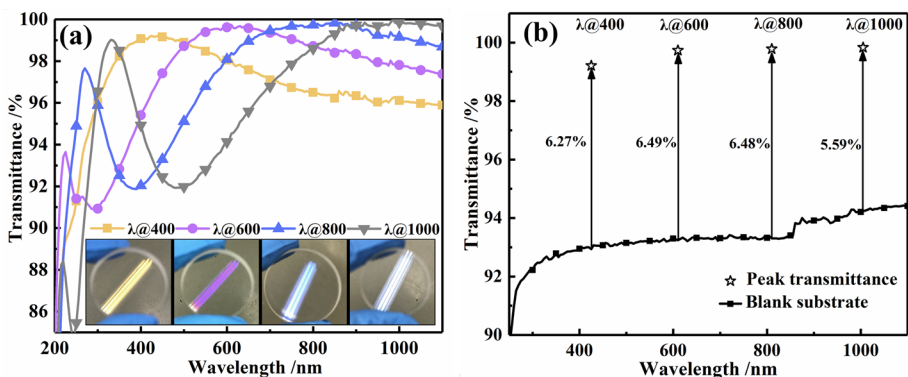

Fig. 3 Optical properties of films: **a** transmittance curves; **b** peak transmittances
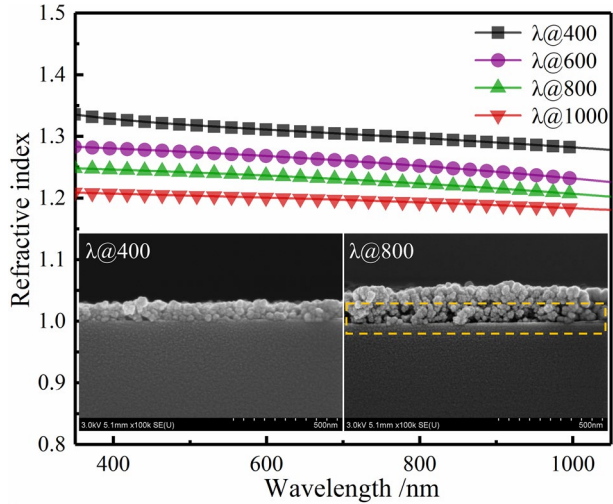
Fig. 4 Refractive index of DLAR films

Table 1 Thickness and porosity of DLAR films

Sample	Measured film thickness /nm	Calculated film porosity /%
λ@400	91.11	25
λ@600	151.93	38
λ@800	198.76	49
λ@1000	245.26	58

The influence of environmental humidity could be reduced by improving the surface hydrophobicity of the films. The surface morphology of the film has a large effect on water repellence as well as on light scattering on a surface. Generally, the affinity of film surface to liquids is manifested in the contact angle, and the larger the contact angle, the smaller the affinity(Xu et al. 2003; Yan et al. 2007).The contact angles between the film and water, corresponding to each coating substrate, were measured using an OCA 40 optical contact angle system (Dataphysics Instruments, Germany). These measurement results are shown in Fig. 5. The water contact angles (WCAs) of the substrates coated with DLAR films were significantly improved compared with the single layer silica antireflective films, and all the WCAs of DLAR films reached approximately 118°. This is because the surface film structures were dense and contained many hydrophobic groups (Fig. 5b), as analyzed using an iS10 FT-IR spectrometer (Nicolet, USA). The absorption peaks at approximately 2973 and 1269 cm^{-1} belonged to the CH_3 group of Si-CH_3.

The coating substrates were placed in a closed environment saturated with potassium sulfate (humidity ˃90%) for 14 d, and the contact angles between the films and water were measured. The measurement results are shown in Fig. 6. Although the coated components were placed in a high humidity environment for a long time, each substrate with films was observed to maintain good hydrophobic properties, with a WCA ˃90°. While the WCA decreased with the thickness increase of the films. It might be that as the thickness of the film increased, there were more tiny pores made it easier for water vapor to penetrate into
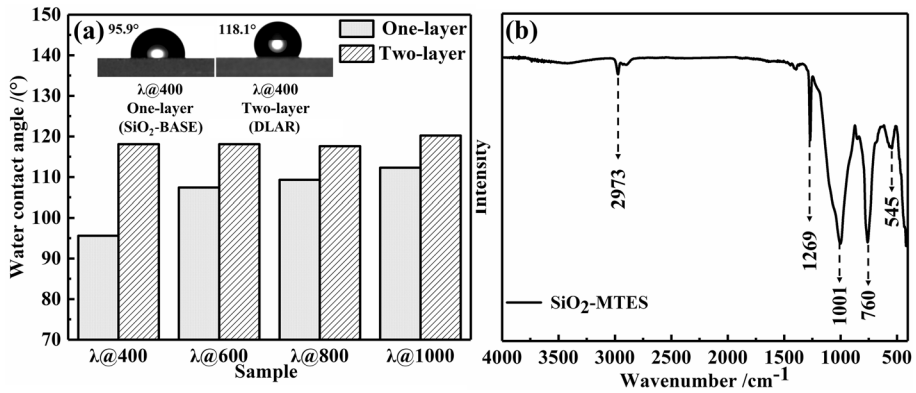
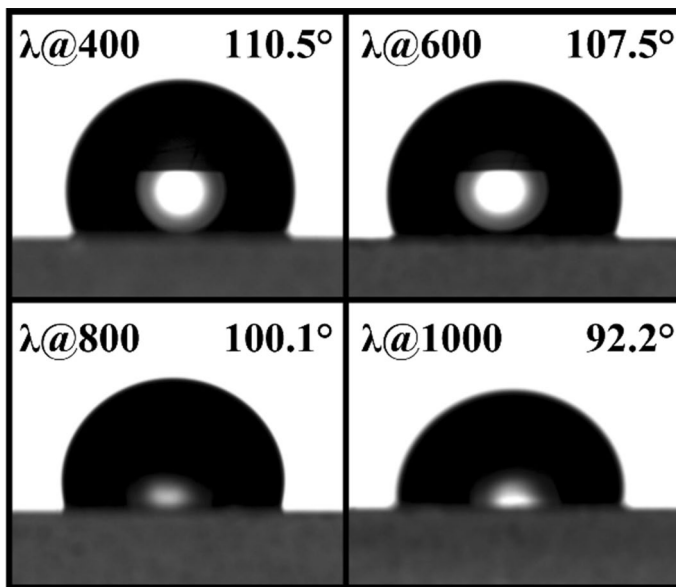**Fig. 5** Hydrophobic properties of films: **a** WCAs; **b** infrared spectrum

Fig. 6 WCAs of films after 14 d in 90% relative humidity

the interior of film, thereby reduced the contact angle. The surface films with dense methyl hydrophobic groups exhibited a good sealing effect and an ability to resist water vapor. In short, the films exhibited good stability.

The surface quality of optical components should be good to ensure stable operation of the laser system under high-throughput conditions and achieve ideal beam-focusing quality, and a smooth surface is beneficial for improving the beam quality. The surface morphologies of the composite film layers were observed using a Dimension 3100 (Veeco, USA) atomic force microscope (AFM). The corresponding results are shown in Fig. 7. The surface roughness (Ra) values of λ@400, λ@600, λ@800, and λ@1000 were 0.71, 1.02,

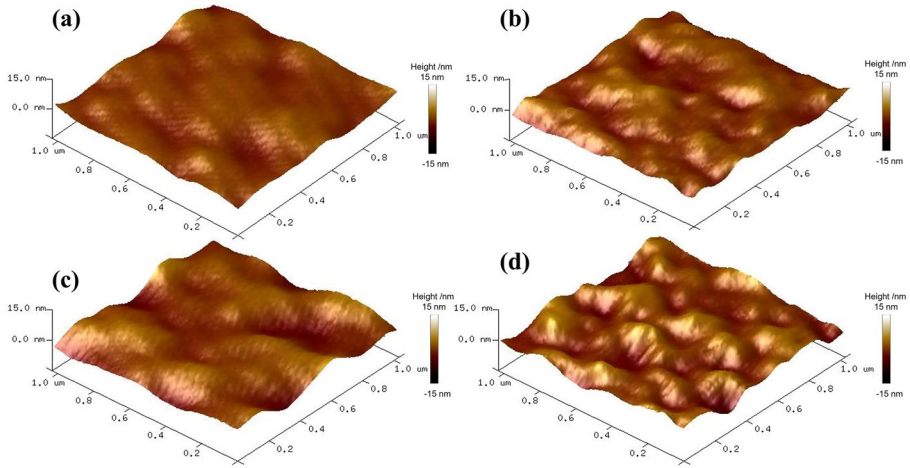**Fig. 7** AFM of films: **a** λ@400; **b** λ@600; **c** λ@800; **d** λ@1000

1.27, and 1.40 nm, respectively, which seemed so helpful to form high-quality light beams. The surface smoothness of the DLAR films was very high, and no prominent burr spikes were observed. Besides, as observed, the λ@400 film exhibited the smoothest surface, and the roughness of the films increased with the increase in the film thickness. This is because when the bottom films were coated with the same concentration of solution, the thickness of the films increased with an increase in the pulling speed within a certain range of pulling speed. The decrease in the deposition time of the colloidal particles resulted in a poor ordered arrangement of particles and a higher film roughness(Zhang et al. 2014).

A scratch resistance testing method was adopted to verify the mechanical properties of the DLAR films to better understand the feasibility of their practical application(Floch et al. 1994). A positive pressure of 0.49 N was applied to the surface of the membrane layer, and the coated substrates were repeatedly wiped with a Micro Denier Winer PRT 2091 silk fabric, shown in Fig. 8, and the surface conditions of the membrane layer observed using a DM4000 metallographic microscope (Leica, Germany). The changes in the sample transmittance before and after wiping were compared and summarized in Table 2. A few
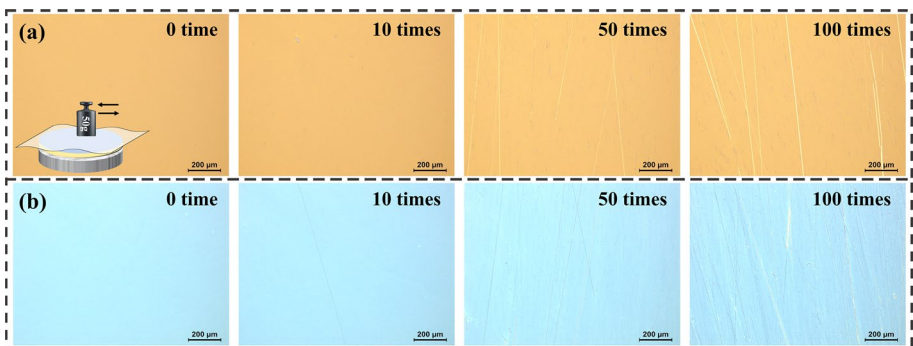

Fig. 8 Schematic diagram of friction experiment and changes in surface morphologies of films after friction experiments

Table 2 Changes in the transmittance of the films

Sample	Peak transmittance /%	Peak transmittance decreased after rubbing /%		
		10 times	50 times	100 times
λ@400	99.06	0.23	0.64	0.79
λ@800	99.70	0.18	0.30	0.76

clear scratches appeared on the film surfaces after more than 50 rounds of back-and-forth friction. This indicated the significantly enhanced strength and good scratch resistance of the DLAR films. The improvement in this performance makes the film layer of the coated components less prone to damage during use and improves the efficiency of the film layer. When the rounds of back-and-forth friction was 10 and 50 times, the peak transmittances of the λ@800 film layer decreased by 0.18% and 0.30%, respectively, while the λ@400 film layer decreased by 0.23% and 0.64%, respectively. The dense layer on the surface has a better protective effect on the relatively thick film layer when the film layer undergoes less times friction.

Laser induced damage to HPLFs is the factor that limits the increases in power and energy(Bouyer et al. 2023). The sol gel silica antireflective film exhibited excellent LIDT, an important indicator for evaluating the performance of the film owing to its porosity. The LIDTs of the films were recorded by test platform at the Shanghai Institute of Optics and Fine Mechanics by the "1-on-1" method(Lian et al. 2020; Lin et al. 2022). The corresponding results are shown in Fig. 9. The optical elements applied on the terminal of HPLFs need to be coated with sol gel chemical films with different requirements, which can play an antireflective effect at specific wavelengths. Finally, the laser physics experiments could complete by converting the harmonic frequency light with a central wavelength of 1053 nm into a third harmonic light with a central wavelength of 351 nm. Therefore, the LIDTs of the substrates with different thickness of DLAR films were tested and the results were 14.9 ± 2.1 J/cm^2 (λ@400, 355 nm, 3 ns), 25.6 ± 3.8 J/cm^2 (λ@600, 532 nm, 3 ns), 35.3 ± 5.3 J/cm^2 (λ@800, 1064 nm, 3 ns), and 45.7 ± 6.9 J/cm^2 (λ@1000, 1064 nm, 3 ns).
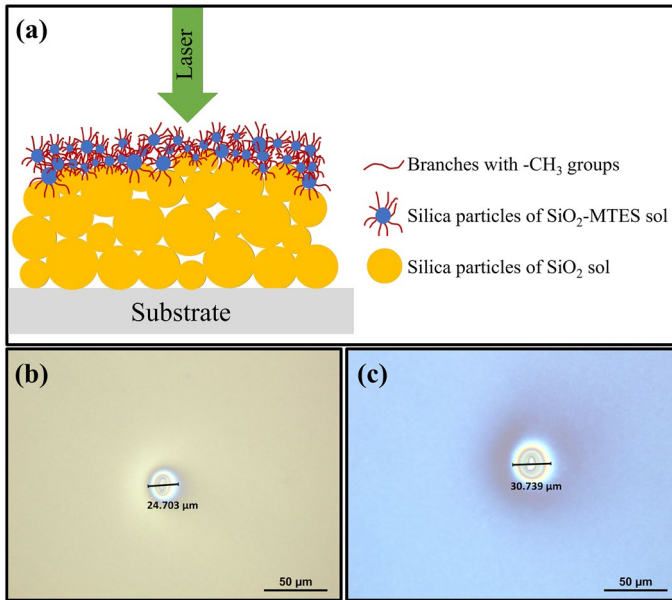
Fig. 9 LIDT of films
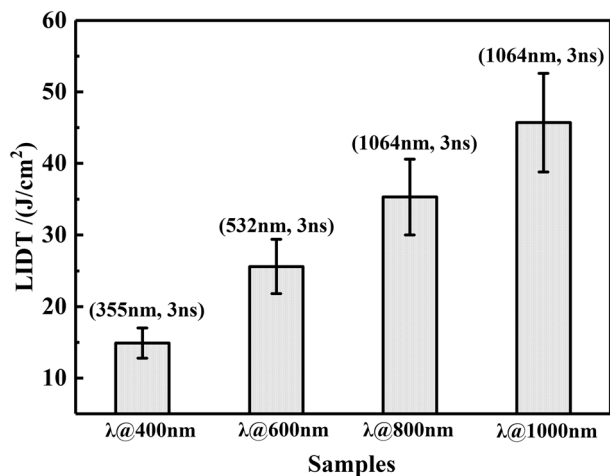
Fig. 10 **a** Schematic of laser damage resistance of DLAR films; **b** damage morphology of λ@400; **c** damage morphology of λ@800

Combined with the LIDT performance results of the sol gel silica antireflective films in different laser facilities(Zhu 2021), the DLAR films with high strength and rubbing resistance were concluded to meet the requirements of HPLFs. The entire structure of the DLAR films maintained the porous and loose structures to form a solid skeleton of all pore walls, as shown in the schematic of the laser damage resistance of DLAR films in Fig. 10a. The thermal energy of the laser rapidly propagated through the hole wall upon the irradiation of films with a laser. The pores between the accumulated particles in the films form a delaying effect and play a role in energy storage. The typical morphology of DLAR films after laser damage is shown in Fig. 10b and c. The morphology is characterized by the formation of concentric damage zones (25–30 μm) around the melting damage spots on the substrate, and the slight gradient discoloration in the films near the damage zones indicates strong compression on the films at the moment of laser damage.

4 Conclusion

Double layer based catalytic silica antireflective films were prepared according to the Stöber method based on SG II HPLF. High-strength films with excellent optical and LIDT properties, owing the dense film layer on the surface, were obtained, which could meet the application requirements of different wavelength antireflective optical elements for HPLFs. In particular, when the antireflective wavelengths of the DLAR films exceeded 600 nm, the overall performance improved. The high strength of antireflective films improves the

damage resistance of the film during use. This can extend their service life and provides a research direction for the preparation of high-performance sol–gel hard films.

Author contributions Bin Shen and Xu Zhang conducted the experiment and data processing. Haiyuan Li and Xinglong Xie provided relevant guidance work. Bin Shen wrote the main manuscript text. All authors participated conceptualization and reviewed the manuscript.

Data availability The data supporting the findings of this study are available from the corresponding author upon reasonable request.

Declarations

Conflict of interest The authors have no conflicts to disclose.

References

Aegerter M. A.: Aerogels Handbook. Springer (2011)

Aegerter M. A., Menning M.: Sol-gel technologies for glass producers and users(Kluwer Academic Publishers) (2004)

Avice, J., Brotons, G., Ruello, P., et al.: Vapor phase ammonia curing to improve the mechanical properties of antireflection optical coatings designed for power laser optics. Gels **9**(140), 9020140 (2023)

Barton, I., Matejec, V., Podrazky, O.: Capillary optical fibers based on SiO_2-TiO_2-P_2O_5 and TiO_2-P_2O_5 internal coatings prepared by sol-gel method. J. Sol-Gel Sci. Technol. **106**, 847–859 (2023)

Boudot, M., Gaud, V., Louarn, M., et al.: Sol-gel based hydrophobic antireflective coatings on organic substrates: a detailed investigation of ammonia vapor treatment(AVT). Che. of Mat. **26**, 1822–1833 (2014)

Bouyer, C., Parreault, R., Roquin, N., Natoli, J.Y., Lamaignère, L.: Impact of temporal modulations on laser-induced damage of fused silica at 351 nm. High Power Laser Sci Eng **11**, e15 (2023)

Chen, Y.G., Lin, Z.Q., Wang, Y.F., et al.: Nd^{3+}-doped silica glass and fiber prepared by modified sol-gel method. Chin. Opt. Lett. **20**(9), 091601 (2022)

Chi, F.T., Zeng, Y.Y., Liu, C., et al.: Aggregation of silica nanoparticles in sol−gel processes to create optical coatings with controllable ultralow refractive indices. App. Mat. & Int. **12**, 16887–16895 (2020)

Cruz, M.E., Castro, Y., Duran, A.: Transparent oxyfluoride glass-ceramics obtained by different sol-gel routes. J. Sol-Gel Sci. Technol. **102**, 523–533 (2022)

Dong, X.S., Mamat, M., Baikeli, Y., et al.: Effect of Fe doping on crystalline phase, structure and photocatalytic properties of TiO_2 thin films. Opt. Mat. **150**, 115196 (2024)

Floch, H., Belleville, P., Pegon, P.: Sol-gel broadband antireflective coatings for advanced laser-glass amplifiers. Proc. SPIE **2288**, 15–24 (1994)

Jiang, H.Y., Zheng, W., Hai, O., et al.: Preparation of hydrophobic anti-reflective silica film with low refractive index. Jou. of Mat. Sci. & Eng. **35**(2), 224–227 (2017)

Li, X.G., Shen, J.: A scratch-resistant and hydrophobic broadband antireflective coating by sol-gel method. Thin Solid Films **519**, 6236–6240 (2011)

Lian, Y.F., Cai, D.T., Sui, T.T., et al.: Study on defect-induced damage behaviors of ADP crystals by 355 nm pulsed laser. Opt. Exp. **28**(13), 18814 (2020)

Lin, X.K., Zhao, Y.A., Liu, X.F., et al.: Damage characteristics of pulse compression grating irradiated by a nanosecond laser. Opt. Mat. Exp. **12**(2), 643–652 (2022)

Liu, B.T., Yeh, W.D.: Antireflective surface fabricated from colloidal silica nanoparticles. Colloids Surf. a: Physicochem. Eng. Aspects **356**(1–3), 145–149 (2010)

Peng, K., Chen, E., Zhou, L.P., et al.: Effects of catalyst on the transmittance and stability of SiO_2 antireflective film prepared by sol-gel method. Adv. Mat. Res. **834–836**, 462–465 (2014)

Shen, B., Li, H.Y., Xiong, H., et al.: Study on low-refractive-index sol-gel SiO_2 antireflective coatings. Chin. Opt. Let. **14**(8), 083101 (2016)

Shen, B., Xiong, H., Zhang, X., et al.: Post-treatment of 351 nm SiO_2 antireflective coatings for high power laser systems prepared by the sol-gel method. Chin. Opt. Lett. **20**(1), 011601 (2022)

Shen, B., Zhang, X., Xiong, H., et al.: Preparation and optical properties of sol-gel SiO_2 antireflective films. Jou. of Ino. Mat. **39**(5), 525–530 (2024)

Sun, J.H., Cui, X.M., Zhang, C., et al.: A broadband antireflective coating based on a double-layer system containing mesoporous silica and nanoporous silica. Jou. of Mat. Che. c. **3**, 7187–7194 (2015)

Tamar, Y., Kahanov, M., Haspel, C., et al.: Size selectivity during dip coating of sol–gel silica-based antireflective coatings and its effect on the porosity of the coatings. Jou. Coa. Tec. Res. **13**(6), 1103–1113 (2016)

Tran, T.N.L., Szczurek, A., Carlotto, A., et al.: Sol-gel-derived transparent glass-ceramics for photonics. Opt. Mat. **130**, 112577 (2022)

Xu, Y., Fan, W.H., Li, Z.H., et al.: Antireflective silica thin films with super water repellence via a solgel process. App. Opt. **42**(1), 108–112 (2003)

Yan, L.H., Chi, F.T., Jiang, X.D., et al.: Preparation of hydro-oleophobic silica antireflective coating. Jou. of Ino. Mat. **22**(6), 1247–1250 (2007)

Ye, H.P., Zhang, X.X., Zhang, Y.L., et al.: Preparation of antireflective coatings with high transmittance and enhanced abrasion-resistance by a base/acid two-step catalyzed sol–gel process. Sol. Ene. Mat. & Sol. Cel. **95**, 2347–2351 (2011)

Ye, L.Q., Ge, X.M., Wang, X.C., et al.: Design and preparation of durable double-layer non-quarter-wave antireflective coatings. Cer. Int. **45**, 8504–8509 (2019)

Yuan, Y., Lu, X.D., Yan, G.H., et al.: Sol-gel preparation of antireflective coatings with abrasion resistance by base/acid double catalysis and surface treatment. Sol. Ene. **155**, 1366–1372 (2017)

Zhang, R.D., Yan, H.W., Lü, H.B., et al.: Changes of thickness and refractive index of silica sol-gel film by dip coating process. Hig. Pow. Las. and Par. Bea. **26**(7), 072005 (2014)

Zhao, W.P., Jia, H.B., Qu, J.X., et al.: Sol-gel synthesis of TiO_2-SiO_2 hybrid films with tunable refractive index for broadband antireflective coatings covering the visible range. J. Sol-Gel Sci. Technol. **107**, 105–121 (2023)

Zhu, J.Q., Sun, M.Y., Jiao, Z.Y., et al.: Key issues of damage resistance of final optics for ICF high power laser facility. Pro. of SPIE **10898**, 1087807 (2019)

Zhu J. Q.: Design and Development of Large High Power Laser Facility, Shanghai Scientific & Technical Publishers (2021)